Copyright ©JCPDS-International Centre for Diffraction Data 2018 ISSN 1097-0002
Advances in X-ray Analysis, Volume 61

Workshop on Challenges in XRF Analysis for Reliable X-Ray Spectra

Jun Kawai, Kohei Yoshida, and Ryohei Tanaka

Kyoto University, Department of Materials Science and Engineering
Sakyo-ku, Kyoto 606-8501, Japan

E-mail: kawai.jun.3x@kyoto-u.ac.jp

ABSTRACT

The present paper is part of a summary of a workshop at Denver X-Ray Conference 2017 in Big Sky, “Challenges in XRF Analysis: Sample Preparation, Spectral Interpretation, and Soft X-ray Detection” presented by J. Kawai, Kyoto University, for spectral interpretation, S. Ichikawa, Fukuoka University, for sample preparation, and Y. Uehara, Mitsubishi Electric Co., for soft X-ray detection. The present part is limited to the spectral interpretation, with emphasis on how to measure reliable X-ray spectra using conventional X-ray detectors such as SSD, SDD, and proportional counters.

INTRODUCTION

Recently, synchrotron radiation facilities are frequently used for X-ray measurements, where concentric long electric cables are used for transferring the X-ray signal from the detector to the recording instruments. On the other hand, fast digital signal processors (DSP) are used in hand-held X-ray fluorescence (HH-XRF) spectrometers for recording the X-ray spectra in place of old analog electric circuits, and therefore the X-ray counting processes are becoming more and more invisible. How to measure a reliable X-ray spectrum will be described for (i) analog circuit of SSD, i.e. old type solid state detectors, (ii) digital SDD (surface or silicon drift detectors) from the view point of sum peaks, and (iii) proportional counters.

ANALOG CIRCUIT OF SSD

Figure 1 shows an example of an old solid state detector, where a liquid nitrogen Dewar vessel is necessary. The detector is under vacuum and cooled down to the liquid

nitrogen temperature to avoid the diffusion of lithium as well as to reduce the electronic noise. However the vacuum seal is in such a way as shown in Fig. 2, and thus vacuum evacuation is needed once every few years to keep the vacuum level. If the vacuum becomes worse, as a result of high voltage (typically 900 V) applied to the detector, electric discharges will happen and the preamplifier is sometimes broken. Even if the vacuum is kept, but such a detector is placed in a high humidity atmosphere like in Japan, the detector window concentrates drops of moisture, and must be kept dry. The plastic bag covering the detector head in Fig. 1 contains silica gel.

Helium is sometimes used for the X-ray path in order to analyze light elements, but the vacuum seal shown in Fig.2 is not suitable for helium, which easily penetrates the vacuum, because of quantum diffusion. This induces electric discharge inside the vacuum vessel. If helium is used, helium diffusion through the O-ring seal must be carefully watched.

Fig. 1. Old solid state detector (Kawai et al. 2005, with permission).

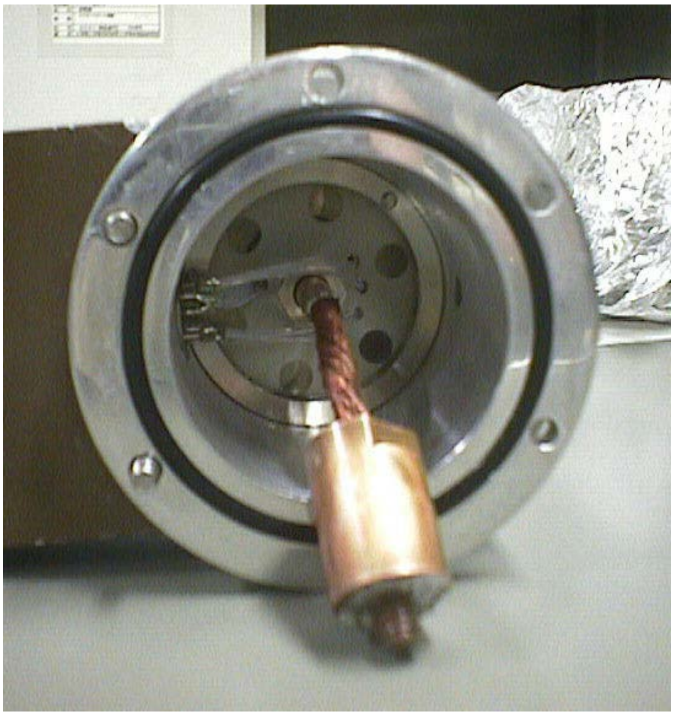

Fig. 2. Inside of Fig. 1 (Kawai et al. 2005, with permission).

Figure 3 compares the two spectra measured by the same Horiba Xerophy pure silicon detector. The sample was a mixture of equimolar V, Mn, Co, and Cu concentration. The top spectrum was measured by the main amplifier condition of integral = 1 μs, 1st differential = 1 μs, and 2nd differential = 0.5 μs. The bottom spectrum was measured by integral =1 μs, 1st differential = 5 μs, and 2nd differential = 1 μs. A small difference of analog amplifier condition changed the relative intensity of four peaks. Careful comparison of the two spectra in Fig. 3 shows additional peaks (e.g. at 8.4 keV), also Kβ peak shifts, and peak broadenings, although the signal to noise ratio was improved. The condition of the top spectrum in Fig. 3 was better than that of the bottom, which was checked by the wave form of the electric signal. The optimum condition should be determined by careful checking of the signal wave form with an oscilloscope.

Copyright ©JCPDS-International Centre for Diffraction Data 2018 ISSN 1097-0002
Advances in X-ray Analysis, Volume 61

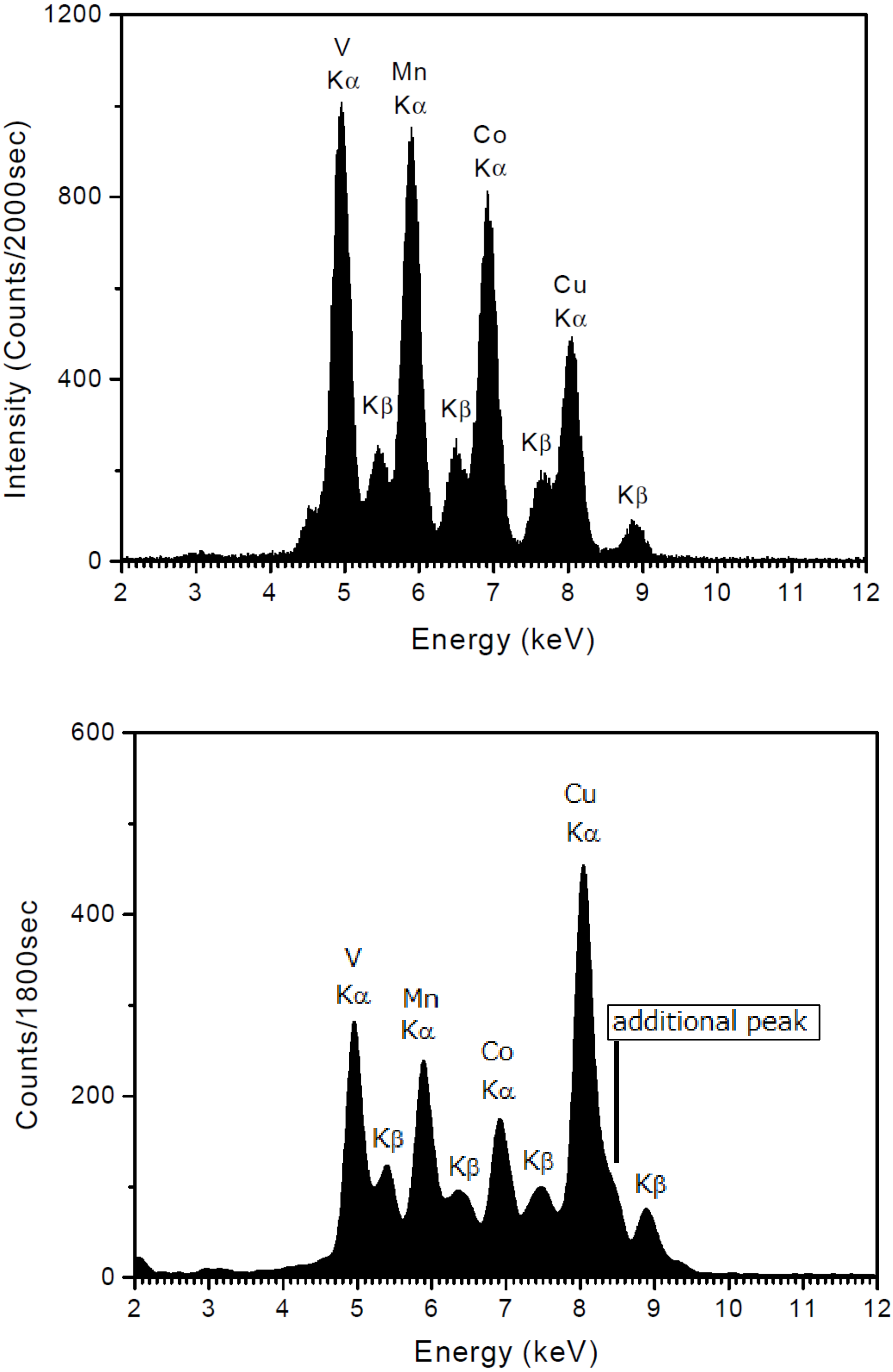

Fig. 3. SSD spectra of the same sample with different circuit parameters (Kawai et al. 2005, with permission).

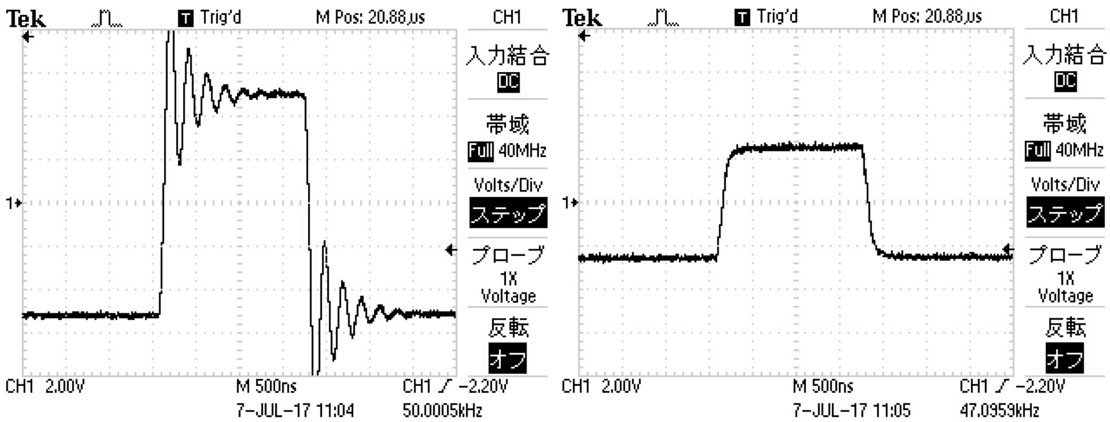

Fig. 4. The electrically bad contact cable (left) without terminator and (right) with a terminator. The length of the cable was 1.5 meters.

Figure 4 shows a bad contact electric cable of length 1.5 meters, which connected a function generator and an oscilloscope. Bending the concentric cable manually resulted in oscillations in the output signal. This means that the electric contact was not good some place in the cable. However, if we insert a terminator, an example of which is shown in Fig. 5, the oscillation disappeared. Inserting a terminator is not the most suitable solution of this fault, instead the bad cable should be replaced by a good one.

Fig. 5. A terminator.

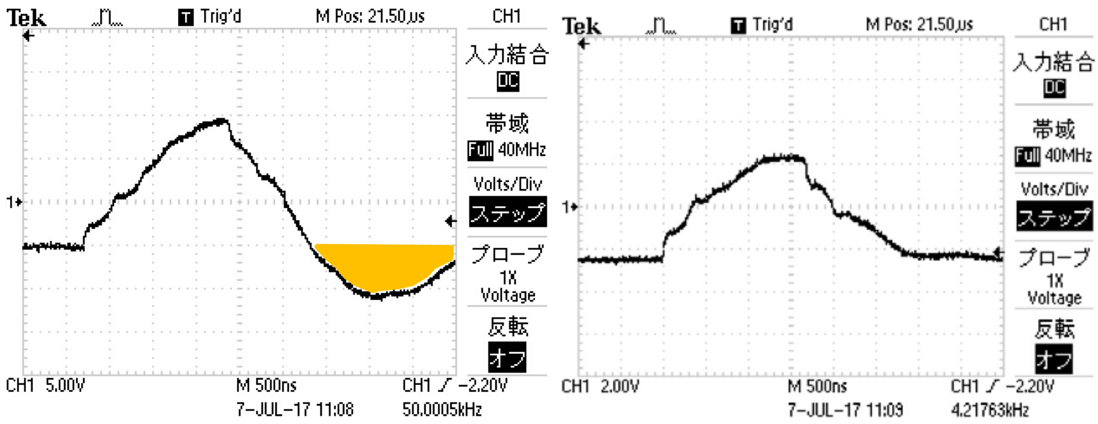

Fig. 6. The electrically bad contact cable (length 1 m) was connected by 60 m cable; (left) without terminator and (right) with a terminator. The color indicate an undershot reflected signal.

Figure 6 shows also the effect of the terminator for a long distance (60 meters) cable. When the distance of the cable increases, the time difference between the true signal and a reflected signal increases, and an undershot signal is separated from the true signal. This undershot signal is a cause of a low energy ghost peak in the EDX spectra. However the best solution is to replace the bad cable by a good one.

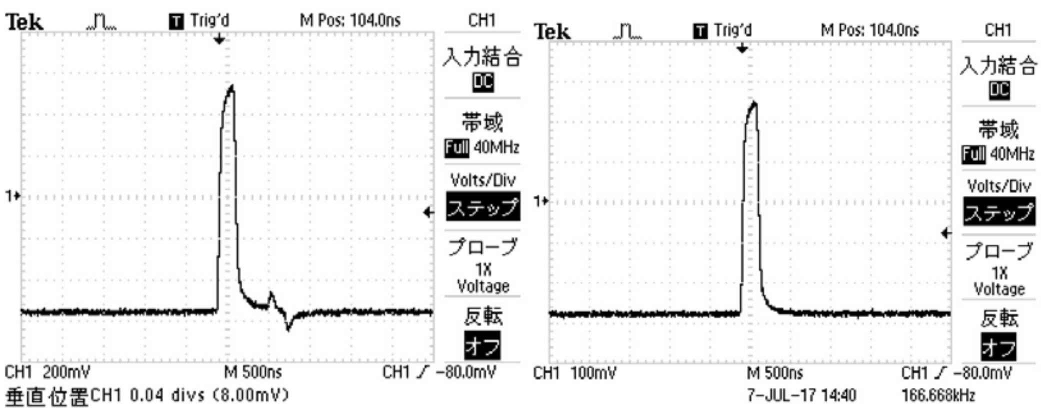

Fig. 7. Two good cables were connected, but the two cables were 73 Ω (3 m length) and 50 Ω (60 m); (left) without terminator and (right) with a terminator. The two cables had no faults.

Copyright ©JCPDS-International Centre for Diffraction Data 2018 ISSN 1097-0002
Advances in X-ray Analysis, Volume 61

Figure 7 also shows an effect of terminator but this time there was no faults with respect to the electric contact, but the impedance was not matched. The signal is reflected at the place where the impedance is mismatched. This kind of undershot signal also causes an artifact X-ray peaks at the low energy side of a strong X-ray peak.

Despite now is an SDD era, and the era of SSD has finished, the thickness of silicon in SSD is thicker than that of SDD, and for higher energy than 20keV X-rays, SSD is still useful. Especially, for much higher energy X-rays, Ge SSD is still in use. From the view point of electric noise, SSD is said to be superior to SDD, and when using SSD, the signal wave before the measurement of the spectra must be carefully checked. However for most of the practical X-ray fluorescence analysis, SDD is better than SSD, because (i) only the detector chip package needs to be under vacuum or sometimes even can be at atmospheric pressure, (ii) the detector does not need to be cooled by liquid nitrogen but only by a Peltier device to about -25 ºC, and (iii) a high voltage is not necessary to be applied.

DIGITAL SIGNAL PROCESSOR (DSP) FOR SDD

The digital signal processor (DSP) is essentially a digital oscilloscope. An analog time line of X-ray pulses is converted into digital signal, and then is processed by a computer. The computer code is usually not open to the users. Therefore, those who are very careful, want to avoid using the DSP, and when using a DSP, analog spectra of the same measurement should be recorded to check the validity of the DSP spectra.

Figure 8 compares the two spectra measured by an analog amplifier and DSP, taken from Tanaka et al. (Tanaka et al. 2017). While the top spectrum is a Ge SSD analog spectrum, the bottom one is an SDD digital spectrum. Both spectra show sum peaks of twice the As and Zn peaks at 21 and 17 keV, respectively. However the details of the line shapes of the two sum peaks are different. The analog sum peak (top) has a low energy tail (indicated by a color triangle to mimic the line shape), but the digital (bottom) has no such a tail (sharp color triangle). The sum peak is the peak of two photons coming at the same time into the detector, and when the detector cannot discriminate the two photons, they are recorded as one photon of energy sum. The tail of the analog sum peak is due to a small difference of time. The DSP has its own algorithm to discriminate the small difference of time, and consequently the tail is removed and two photons are added to the single photon peak. This is an example of the difference between an analog amplifier and DSP.

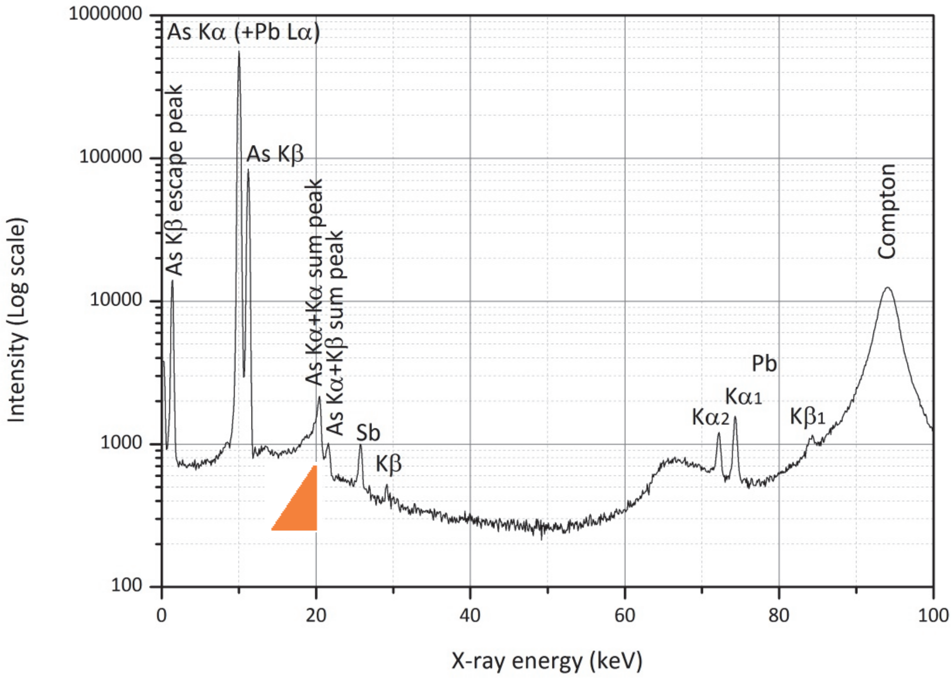

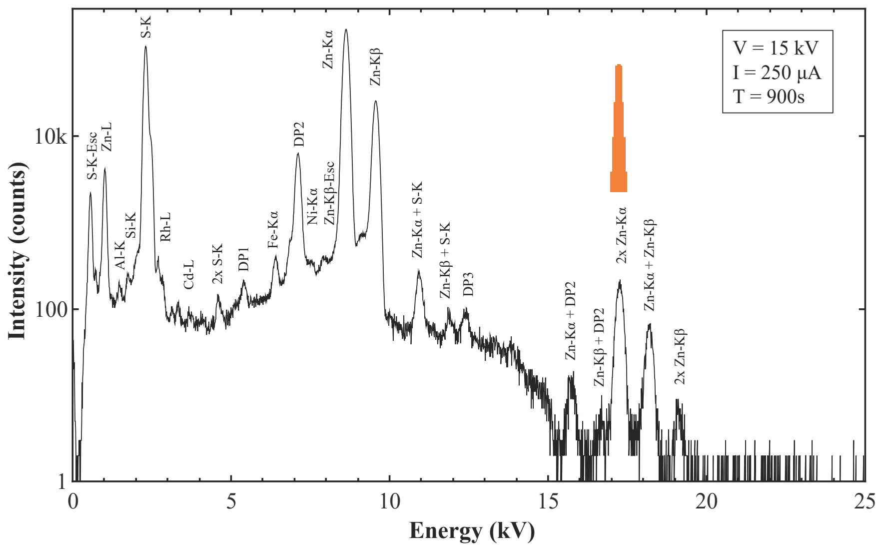

Fig. 8. Comparison of (top) analog spectrum and (bottom) digital spectrum (taken from Tanaka et al. 2017 with permission).

If a fast SDD is used by an analog amplifier, the detector counting rate is not improved, and limited to a similar counting rate of an old analog SSD. The combination of SDD and DSP makes it possible to count with a high counting rates over one million counts per second (cps).

The shaping time of DSP will also limit the counting rate. In other words, if the spectral energy resolution is higher with a long shaping time, the counting rate is limited, and if the spectral resolution is sacrificed by a short shaping time, the high counting rate is achieved. For example, while the shaping time of 0.25 microseconds is equivalent to a 190 eV resolution for Mn for a commercially available SDD, 6 microseconds shaping time is equivalent to 140 eV resolution.

PROPORTIONAL COUNTERS

The proportional counter is an energy dispersive X-ray detector. The energy resolution is not good but energy spectra can be obtained. Figure 9 shows EDX spectra of monochromatic V Kα X-rays measured by a proportional counter. The vanadium $K\alpha_1$ was monochromized by a double-crystal X-ray fluorescence spectrometer (Gohshi et al. 1972), and the proportional counter signals were transferred to and recorded by a pulse height analyzer (PHA). The resolution of the double-crystal spectrometer was less than the natural line width of $K\alpha_1$ peak. The two spectra in Figure 9 were recorded at 67 cps and 998 cps by changing the 2θ angle at $K\alpha_1$ peak and a few eV off from the $K\alpha_1$ peak.

It is remarkable from Fig. 9 that the energy distribution curve is broader for a lower counting rate, and narrower for a higher counting rate, in spite that photon energy is monochromatic (less than 0.1 eV band width but a few eV difference) for vanadium $K\alpha_1$. It can be said that the gas amplification is different depending on the counting rate. This is widely known by X-ray company researchers, but not well known by users. The small peak around 1-3 V is the escape peak due to argon. The distortion of the main peaks (3-8 V) in Fig. 9 was due to an inhomogeneous electric field originated from carbon contamination of the wire. If the wire is cleaned by heating or replaced by new one, the main peak will become symmetric.

Copyright ©JCPDS-International Centre for Diffraction Data 2018 ISSN 1097-0002
Advances in X-ray Analysis, Volume 61

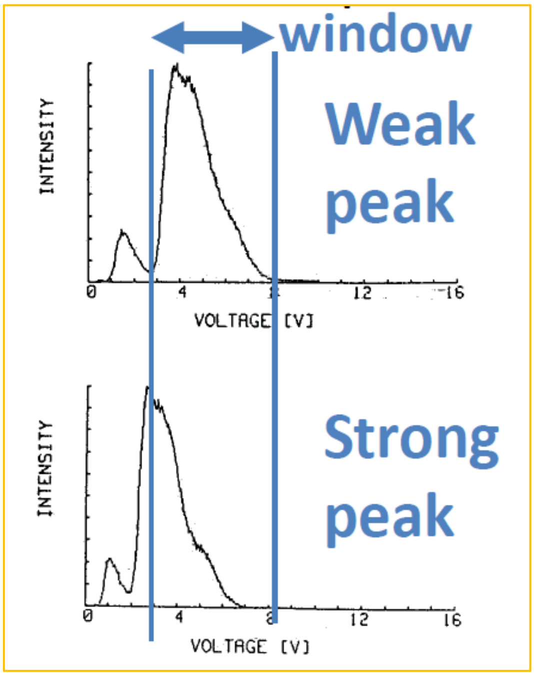

Fig. 9. Proportional counter EDX spectra for monochromized X-rays, in dependency on counting rate: top 67 cps and bottom 998 cps. Spectra were taken from Kawai (Kawai, 1982 and 2004).

If a window of a single channel analyzer (SCA) of the proportional counter of a wavelength dispersive spectrometer is set in such way as indicated by the blue lines in Fig. 9, the vanadium peak signal extended beyond the window as the intensity becomes stronger, and the measured peak intensity becomes lower than the true intensity.

An example is shown in Fig. 10. The two spectra show arsenic evidences of an arsenic murder incidence reported by Kawai (Kawai, 2014) measured by the National Research Institute of Police Science, Japan. The sample amount of the upper spectrum was not enough and thus the spectral intensity was lower than 10 kcps. Another sample amount was enough and the spectral intensity was as strong as 100 kcps, as shown at the bottom of Fig. 10. The Kβ/Kα intensity ratios should be the same for these two spectra. However, if Kβ/Kα intensity ratios are compared between the top and bottom of Fig. 10, the bottom Kα intensity seemed to be saturated. This is because the pulse height distribution of intense peak was shifted to the lower energy side and outside of the window of the SCA, other than the insufficient dead time corrections. Consequently, the Kβ intensity of the bottom spectrum becomes relatively stronger than that of the top spectrum.

Copyright ©JCPDS-International Centre for Diffraction Data 2018 ISSN 1097-0002
Advances in X-ray Analysis, Volume 61

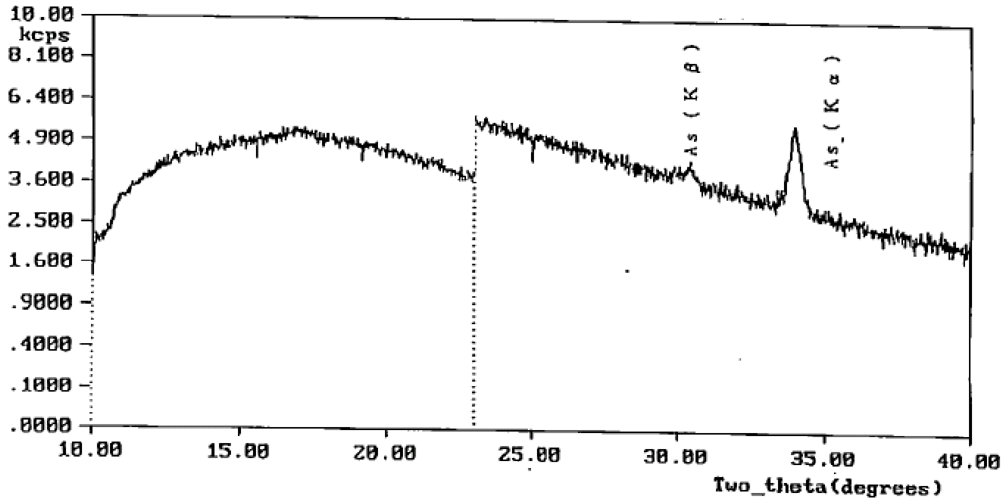

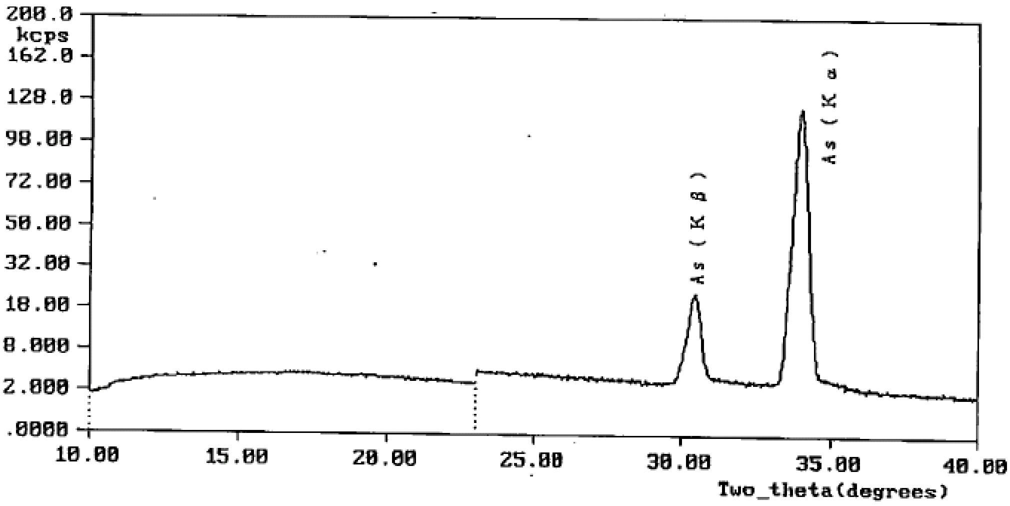

Fig. 10. Arsenic Kβ/Kα intensity difference of murder case evidence (taken from a public document of the National Research Institute of Police Science, Japan, and not a copyrighted matter).

CONCLUSIONS

Some of the techniques in order to measure reliable X-ray fluorescence spectra have been described. Pole zero adjustment has been omitted in the present paper. Most of the analog main amplifiers have small hole indicated by “PZ”, and this is the pole zero adjustment to avoid the undershot of X-ray pulse shown in Fig. 6.

Analog circuits (i) and digital signal processors (ii) for X-ray detectors have been described. Both, the analog and digital circuits should be used simultaneously in order to cross-check a reliable X-ray spectrum at the research stage, as long as the algorithm of the digital signal processor has not been made available to users. The gas amplification change of a proportional counter has been explained, but it should be noted that similar phenomena exist more or less for any kinds of X-ray detectors.

REFERENCES

Gohshi, Y., Hukao, Y., Hori, K. (**1972**). “A wide-range, single-axis, vacuum two-crystal spectrometer for fluorescent X-ray analysis”, Spectrochimica Acta Part B: Atomic Spectroscopy, **27**, 135-142.

Kawai, J. (**1982**). “Studies on the Profile Changes of X-Ray Spectra”, Thesis for Bachelor of Engineering, Advisor: Yohichi Gohshi, The University of Tokyo, DOI: 10.13140/RG.2.2.14702.31044

Kawai, J. (**2004**). “Proportional counters”, Advances in X-Ray Chemical Analysis, Japan, **35**, 209-222.

Kawai, J., Murakami, H., and Koyama, T. (**2005**). “Solid state detector”, Advances in X-Ray Chemical Analysis, Japan, **36**, 189-200.

Kawai, J. (**2014**). “Forensic analysis of arsenic poisoning in Japan by synchrotron radiation X-ray fluorescence”, X-Ray Spectrometry, **43**, 2-12.

Tanaka, R., Yuge, K., Kawai, J., and Alawadhi, H. (**2017**). “Artificial peaks in energy dispersive X-ray spectra: sum peaks, escape peaks, and diffraction peaks”, X-Ray Spectrometry, **46**, 5-11.